In the present study, we used the cysteine-scanning spin-labeling method to analyze the dynamics of recombinant moPrP mutants that were singly labeled at 17 residues in α-helix1 (H1, codon 143–151), β-sheet1 (S1, codon 127–130), and β-sheet2 (S2, codon 160–163). We determined the locations of the pH-sensitive protein sequences in the H1 and S2 regions.

Materials and methods

Materials. (1-Oxy-2,2,5,5-tetramethyl-3-pyrroline-3-methyl) methanethiosulfonate (MTSSL) was purchased from Toronto Research Chemicals (ON, Canada). *Escherichia coli* BL21(DE3)LysS and isopropylthio-β-D-galactoside (IPTG) were from Invitrogen (CA, USA). Ni Sepharose 6 Fast Flow was from Amersham Biosciences Co. (NJ, USA). The TSKgel Phenyl-5PW RP column was from TOSOH (Tokyo, Japan). The Protein Assay Lowry Kit was from Nacalai Tesque, Inc. (Kyoto, Japan). 2-[4-(2-Hydroxyethyl)-L-piperazinyl]ethanesulfonic acid (HEPES) and 2-morpholinoethanesulfonic acid, monohydrate (MES) were from Dojindo, Lab. (Kumamoto, Japan). Other reagents were from Wako Pure Chemical, Co. (Tokyo, Japan).

Construction of moPrP mutants. cDNA encoding mouse PrP (residues 23–231) was cloned into *Bam*HI/*Eco*RI sites of pRSETb as described previously [22,23]. In the plasmid encoding moPrP, single amino acids at H1, S1, and S2 were substituted for by cysteine residues (Fig. 1A). These moPrP mutants were generated by the PCR-based site-directed mutagenesis method [22,24]. Oligonucleotides used in the mutagenesis were obtained from Sigma Genosys. The change of the target codons by cysteine residues was confirmed using a CEQ8800 automated sequencer (Beckman Coulter, Inc.).

Expression and purification of recombinant moPrP mutants. The expression and purification of recombinant moPrP mutants were modified from those described previously [22]. The expression plasmids were introduced into *E. coli* BL21(DE3)LysS. *E. coli* BL21(DE3)LysS with each moPrP construct was grown overnight in 100 ml SOB liquid culture medium containing 1% sucrose, 0.1 mg/ml ampicillin, and 0.05 mg/ml chloramphenicol at 37 °C. Then 15 ml of overnight culture was added to 450 ml SOB medium with 1% sucrose, 0.1 mg/ml ampicillin, and 0.05 mg/ml chloramphenicol and grown at 37 °C to an optical density at 600 nm of 0.7. Protein expression was induced by adding IPTG to a final concentration at 0.5 mM. The culture was continued for 7 h and then bacterial cells were collected by centrifugation. The bacterial pellets were suspended in 6 M GdnHCl in 20 mM Na_2HPO_4 (pH 7.8) and sonicated to completely release the inclusion bodies from BL21(DE3)LysS transformed with expression plasmids. Separated inclusion bodies in 6 M GdnHCl in 20 mM Na_2HPO_4 (pH 7.8) were incubated with Ni^{2+}-charged chelating Sepharose for 1 h to purify the recombinant moPrP. The protein-bound Sepharose was washed 2× with 8 M urea in 10 mM Tris/HCl and 100 mM NaH_2PO_4 (pH 6.2), and then loaded into the column. The recombinant moPrP was eluted using 8 M urea in 10 mM Tris/HCl and 100 mM NaH_2PO_4 (pH 4.2). After dialysis against 10 mM acetate buffer (pH 4.0) for 48 h, recombinant moPrP was purified by reverse-phase high performance liquid chromatography (HPLC) using TSKgel Phenyl-5PW RP and a 40–60% linear gradient of acetonitrile with 0.05% trifluoroacetic acid. The purified recombinant moPrP was dialyzed against 10 mM acetate buffer (pH 4.0) for 48 h, concentrated with a centrifugal concentrator (Vivascience) to approximately a quarter of its original volume, and then stored at −80 °C until use. The protein concentration was quantified with the Lowry protein assay using BSA as a standard [25]. The final protein purity (>98%) was confirmed by sodium dodecyl sulfate polyacrylamide gel electrophoresis (SDS–PAGE) and Coomassie brilliant blue staining.

Spin-labeling of moPrP mutants. To label the moPrP mutants with MTSSL, a 10-fold molar excess of MTSSL was added to each protein and incubated overnight in the dark at 4 °C. The free MTSSL was removed from the protein using a microdialyzer (Nippon Genetics). To confirm that the α-helix content of spin-labeled moPrP mutants was similar to that of wild-type moPrP, we used a far-UV CD spectropolarimeter (J-820, JASCO) [22]. The sample was diluted to 0.3 mg/ml protein concentration and scanned using a scan speed of 50 nm/min and a response time of 2 s. In all mutants, the two minima (208 and 220 nm), typical of a mainly α-helix-structure protein, were clearly observed and there were no differences in the α-helix content between wild-type moPrP and spin-labeled moPrP mutants [22,26].

ESR spectroscopy. Details of the ESR spectroscopy methods have been published elsewhere [22]. The pH change of the sample solution was carried out by dialysis of the sample against the three buffers, 10 mM acetate buffer (pH 5.0), 10 mM MES buffer (pH 6.4), and 10 mM Hepes buffer (pH 7.4). ESR spectra were recorded in a quartz flat cell (RST-DVT05; 50 mm × 4.7 mm × 0.3 mm, Radical Research) for spin-labeled samples of 20 μM moPrP using a JEOL-RE X-band spectrometer (JEOL) with a cylindrical TE011 mode cavity (JEOL). All ESR spectra were obtained at 20 °C, controlled by a temperature controller (ES-DVT4, JEOL), under the following conditions: 5 mW incident microwave power, 100 kHz modulation frequency, 0.2 mT field modulation amplitude, and 10 mT scan range. The $1/\delta H_0$ of the central component (M_I=0: ^{14}N hyperfine) in the ESR spectrum of spin-labeled $moPrP^C$ was employed as a mobility parameter and was further analyzed using a Win-Rad Radical Analyzer System (Radical Research). To reveal the motional change upon pH variation, we further examined the second moment $\langle H^2 \rangle$, a measure of spectral deviation due to the motional narrowing (or broadening) of ESR spectra. The second moment was estimated numerically with the Win-Rad System.

Results

Mobility change with pH: ESR spectral features from $moPrP^C$

Fig. 2A shows the ESR spectra from recombinant full-length moPrP mutants in the H1 region at pH 7.4 at 20 °C. Each ESR spectrum from the nine mutants in the H1 region of moPrP showed a different line shape (Fig. 2A). In general, the ESR spectra from H1 region indicate mobile signals with small immobile contributions. The ESR spectra obtained from E145R1 and Y149R1 showed line broadening as compared with those of D143R1 or R150R1, indicating the immobility of the nitroxide probe in E145R1 and Y149R1. To obtain detailed mobility information, we measured the inverse of the peak-to-peak first derivative width of the central resonance ($1/\delta H_0$) in each ESR spectrum in the H1 region, since it has been reported by Hubbell et al. that $1/\delta H_0$ from the ESR spectrum as a mobility parameter is strongly correlated with the local environment of the protein domain structure [17]. The values of $1/\delta H_0$ obtained from the ESR spectra of D143R1, R147R1, R150R1, and E151R1 were approximately 4.07, 2.82, 3.50, and 3.35, respectively. On the other hand, those obtained from the ESR spectra of E145R1 and Y149R1 were approximately 2.19 and 2.75, respectively. The plotted data of $1/\delta H_0$ shown in Fig. 2B indicate the periodical changes in the H1 region. In the S1 region, the ESR spectrum of M129R1 was slightly narrower than those of the other positions in S2 (Fig. 3A) and the $1/\delta H_0$ (3.20) of the M128R1 mutant was slightly higher than those of Y127R1 (2.86), L129R1 (2.88), and G130R1 (2.84) (Fig. 3B). In the S2 region, there were no differences in the line shapes of the ESR spectra of V160R1, Y161R1, Y162R1, and R163R1 (Fig. 4A), and the values of $1/\delta H_0$

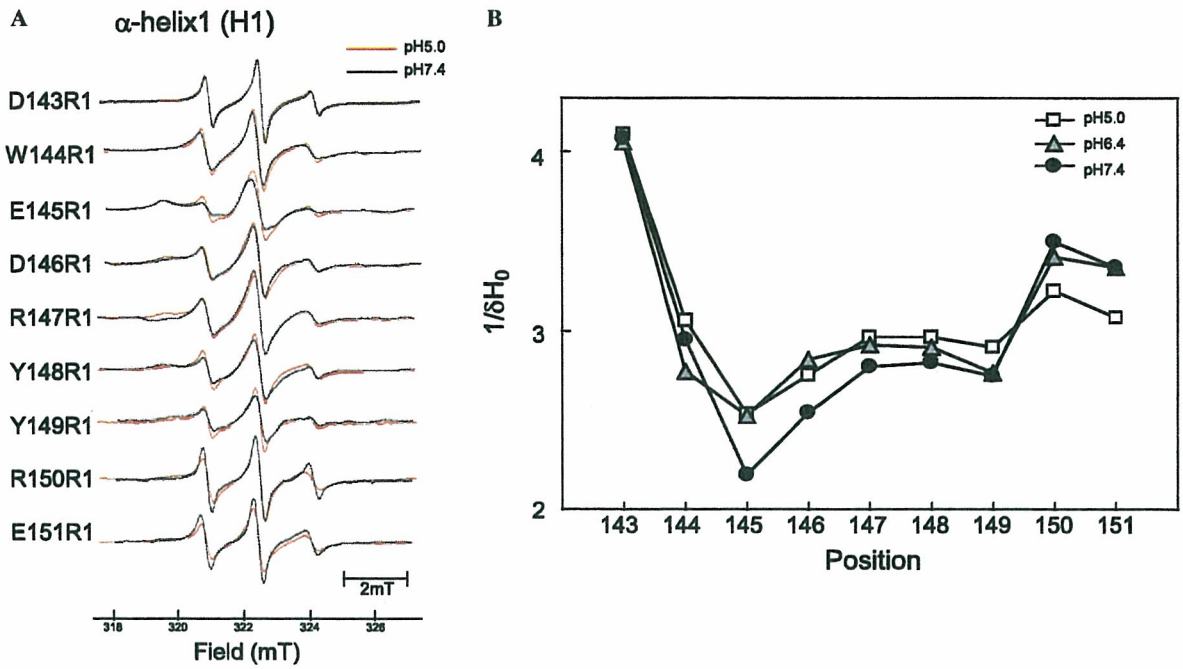

Fig. 2. ESR spectra of α-helix1 (H1) mutants and effects of pH on their line shapes. (A) ESR spectra of nine moPrP mutants at pH 7.4 (black line) and pH 5.0 (red line) were recorded using an X-band ESR spectrometer at 20 °C. (B) The pH-dependent changes in domain mobility of moPrP mutants. The values of $1/\delta H$ obtained from the peak-to-peak central component ($M_I=0$) in the ESR spectra of spin-labeled moPrP^C at H1 were plotted as a function of pH. (For interpretation of the references to colour in this figure legend, the reader is referred to the web version of this article).

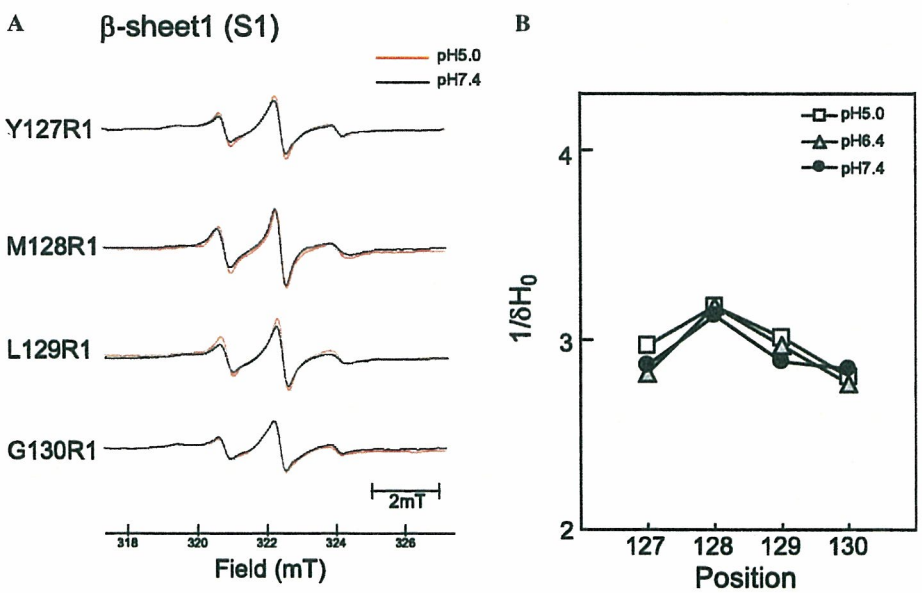

Fig. 3. ESR spectra of β-sheet1 (S1) mutants and effects of pH on their line shapes. (A) ESR spectra of four moPrP mutants were recorded at pH 7.4 (black line) and pH 5.0 (red line) at 20 °C. (B) The values of $1/\delta H_0$ of the nitroxide probes of S1 mutants are plotted as a function of pH. (For interpretation of the references to colour in this figure legend, the reader is referred to the web version of this article).

from the ESR spectra of these four mutants ranged from 2.1 to 2.3, indicating that the nitroxide probes in S2 were strongly immobilized in comparison with those in S1 (Fig. 4B).

pH-induced conformational changes in moPrP^C

Since it has been suggested that acidic pH is involved in the conformational transition from PrP^C to PrP^{Sc} [7–9], we examined the effects of pH changes on the line shapes of ESR spectra of moPrP^C as shown in Figs. 2A, 3A, and 4A. In the H1 region, each mutant showed a different pattern for the variation of the ESR spectrum during the reduction of pH. When pH in the solution decreased from pH 7.4 to pH 5.0 at 20 °C, there was no significant change in the ESR spectrum of D143R1, but the ESR spectrum of E145R1 became narrow, indicating a pH-dependent

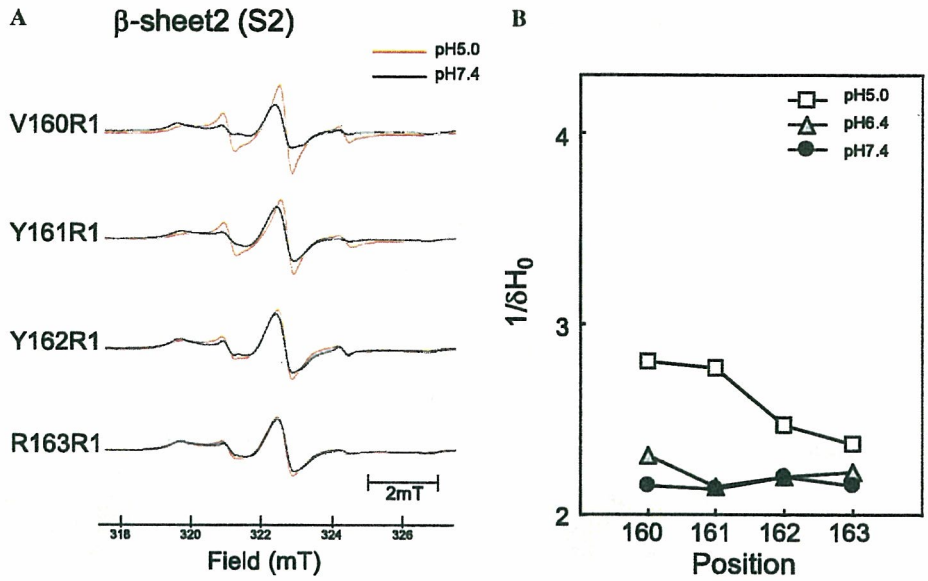

Fig. 4. ESR spectra of β-sheet2 (S2) mutants and effects of pH on their line shapes. (A) ESR spectra of four S2 mutants at 20 °C and pH 7.4 (black line) and pH 5.0 (red line). (B) The values of $1/\delta H_0$ of the nitroxide probes of S2 mutants are plotted as a function of pH. (For interpretation of the references to colour in this figure legend, the reader is referred to the web version of this article).

conformational change from a rigid to a flexible structure. In contrast to this, the decrease of pH-induced line broadening in the ESR spectra of R150R1 and R151R1. In the β-sheet regions, no pH-dependent changes in the line shapes of ESR spectra of S1 were observed (Fig. 3A). However, the decrease of pH-induced narrow line shapes in the ESR spectra of V160R1 and Y161R1 in S2.

Figs. 2B, 3B, and 4B show the pH-dependent changes of $1/\delta H_0$ from ESR spectra in various regions at 20 °C. In the H1 region, the value of $1/\delta H_0$ of D143R1 at pH 5.0 was similar to that of pH 7.4. However the $1/\delta H_0$ of E145R1 increased from 2.2 to 2.5 when the pH in the solution slightly changed from 7.4 to 6.4 and remained constant at the high level of pH 5.0. The values of $1/\delta H_0$ of D146R1 and R147R1 also slightly increased at pH 6.4 in comparison with pH 7.4. In contrast, the values of $1/\delta H_0$ of R150R1 and E151R1 decreased when the pH in the solution decreased from 6.4 to 5.0. On the other hand, the pH-dependent change in $1/\delta H_0$ was not observed in the S1 region. The values of $1/\delta H_0$ of V160R1, Y161R1, Y162R1, and R163R1 in the S2 region increased when pH in the solution decreased from 6.4 to 5.0, but the changes in $1/\delta H_0$ of Y162R1 and R163R1 resulting from a decrease of pH from 6.4 to 5.0 were relatively small.

Discussion

Structural studies by NMR of recombinant hPrP (23–230) [13,27], moPrP (23–231) [28], and hamster PrP (29–231) [29] revealed a highly flexible N-terminal octapeptide repeat region and C-terminal global region. Figs. 5B and C shows global features of the refined NMR structure of the C-terminal globular region, moPrP (121–231), as reported by Riek et al. [30]. Prion proteins in the cell are attached to the plasma membrane via a glycosyl phosphatidylinositol (GPI) anchor and localized in membrane lipid rafts [1,31]. Lipid rafts, which are rich in spingolipids and cholesterol, are associated with endocytosis. Endosomes and lysosomes are typical acidic organelles [32], their luminal pH is formed by vacuolar type proton ATPase (V-ATPase) and varies between 6.5 and 4.5 [33,34]. Many past studies demonstrated the relationship between the pH of intracellular acidic compartments and conversion from PrP^C to PrP^{Sc} [7–16,35]. Recently, the *in vivo* conversion of human brain PrP^C to a PrP^{Sc}-like form was reported to be enhanced at acidic pH [36] and biophysical studies have shown that the free energy of unfolding of hPrP (90–231) is lower at acidic pH than at neutral pH [10]. A β-sheet-rich folding intermediate was observed for moPrP (121–231) at low pH in urea but was also seen at neutral pH [37]. The mechanism for pH-dependent structural changes of prion protein was reported in molecular dynamics (MD) simulation studies [14,15,38]. On the other hand, experimental data about the pH-sensitive region of prion proteins seem to be insufficient although there was one report suggesting that the C-terminal end of Helix1 and 161–164 of S2 have a larger tendency to unfold as revealed by NMR with amide proton protection factor mapping of the globular domain of PrP [16].

The SDSL–ESR technique can be used to analyze high molecular weight proteins for which NMR spectroscopic and X-ray crystallographic methods are not generally applicable [17–20]. In the present study, we employed the SDSL–ESR technique to obtain experimental information on pH-sensitive regions of recombinant $moPrP^C$. Hubbell et al. first used the inverse of peak-to-peak first derivative width of the central resonance ($1/\delta H_0$) of the ESR spectrum as a mobility parameter [17]. We also measured the

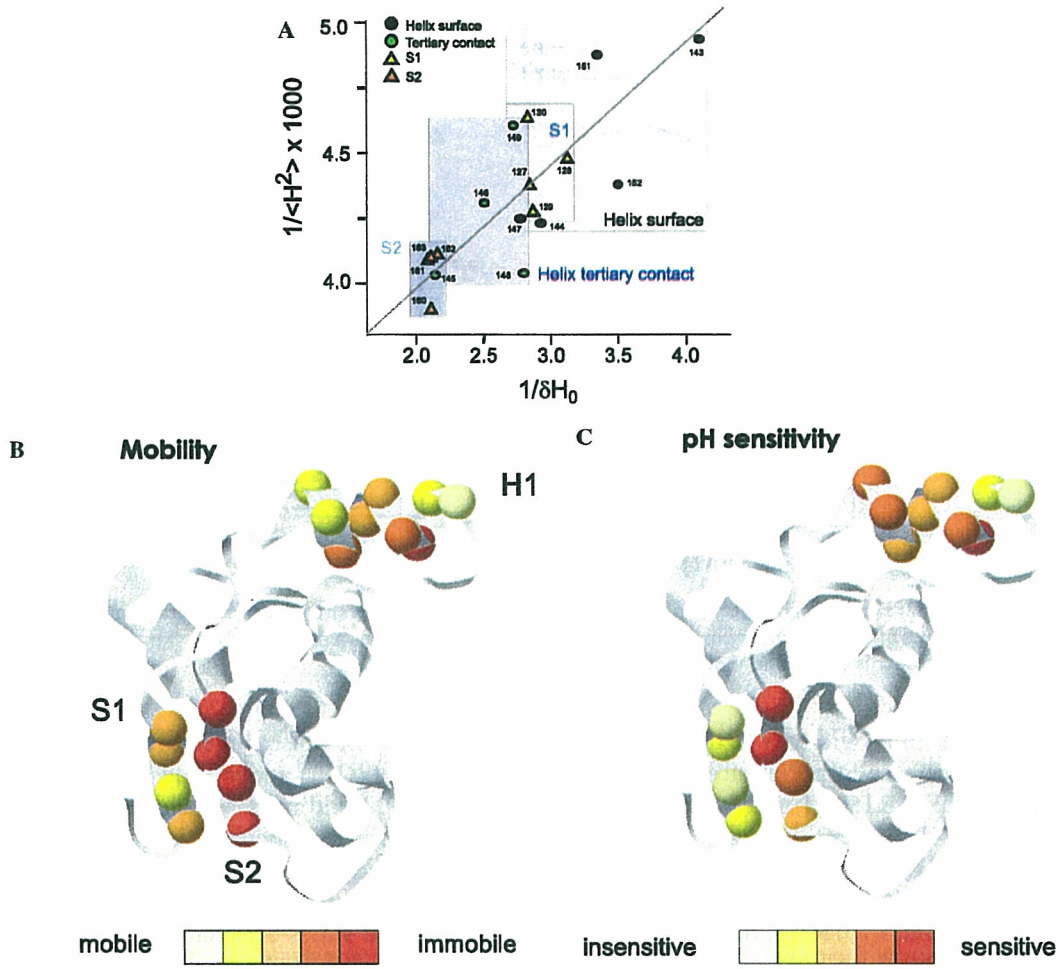

Fig. 5. The dependency of the mobility parameters of the ESR spectrum on the 3D structure of PrP and identification of pH-sensitive regions of PrP. (A) The general relationship between the mobility of the nitroxide side chain and salient features of the moPrP. The inverse spectral second moments ($1/\langle H^2 \rangle$) and the inverse central linewidths ($1/\delta H_0$) for the R1 side chain at 17 sites in moPrP are expressed as semiempirical parameters of mobility. The topographic regions of moPrP were classified into four protein folding categories; i.e., the helix surface site, the helix tertiary contact site, S1 (the surface side), and S2 (the buried side). The light gray line shows the regression linear fitting between these two mobility parameters. The value, r=0.80 (n=17) of Pearson's correlation coefficient obtained from these two parameters, was greater than the 1% significance value, r=0.606 (n=17), indicating that the reciprocal central linewidth was positively correlated with the inverse of the spectral second moments. (B) The variation of mobility obtained from ESR spectra of recombinant moPrP mutants in physiological conditions (pH 7.4). Each α-carbon position indicated by graduated colors for relative mobility was superimposed on the 3D structure of moPrP as reported by an NMR study (PDB entry 1AG2, [28]). (C) The 3D positions of pH-sensitive regions of PrP. The magnitude of mobility change induced by a decrease from pH 7.4 to pH 5.0 was qualitatively evaluated. Each α-carbon indicated by graduated colors for relative pH sensitivity was superimposed on the 3D structure of moPrP as reported by an NMR study [28]. (For interpretation of the references to colour in this figure legend, the reader is referred to the web version of this article).

$1/\delta H_0$ in ESR spectra at pH 7.4 and 20 °C. Figs. 2B, 3B, and 4B show the values of $1/\delta H_0$ obtained from the cysteine-scanning SDSL–ESR data of H1, S1, and S2, respectively. In the H1 region, a periodical change of $1/\delta H_0$ was observed. In comparison with the 3D structure of moPrP as estimated by NMR data, shown in Fig. 5B, highly mobile residues of the nitroxide probe in D143R1, R147R1, and R150R1 were located on the outer surface of H1, whereas low mobility residues such as E145R1 and Y149R1 were in the inner contact residues of H1. These variations of mobility in the nitroxide probe were well correlated with the 3D helix structure of moPrP. On the other hand, the fluctuation in the values of $1/\delta H_0$ of the S1 region in neutral pH solution of moPrP was small, although the value at M128R1 was observed to be relatively high (Fig. 3B). Furthermore, the values of $1/\delta H_0$ of the S2 region were lower than those of the S1 region (Figs. 3B and 4B). The 3D structure of moPrP identified by NMR (Fig. 5B) showed that the S2 region was located in the buried structure close to H2 and H3, whereas the S1 region was located in the relatively outer side of moPrP. The difference of mobility between S1 and S2 regions can probably be explained by the difference of the tertiary structure of moPrP. To define the relationship between structure and mobility, with the aid of $1/\delta H_0$, it is convenient to employ a further semiempirical parameter for mobility reflected in ESR spectra: namely the spectral breadth, which is represented by the spectral second moment

($<H^2>$) [39]. The numerical values of these quantities are mainly determined by the degree of averaging of magnetic tensor values. As the frequency of nitroxide rotational motion is lowered, the second moment and the line width increase. Fig. 5A shows a plot of the reciprocal second moment ($1/<H^2>$) versus the reciprocal central line width ($1/\delta H_0$) for the spectra of R1 side chains representing the helix surface, helix tertiary contact, and two β-sheets (S1 and S2). As shown in Fig. 5A, the mobility was consistent with the tertiary fold of moPrP and there was a linear correlation between these two parameters. These results indicated that these parameters were related to the 3D structure of PrP.

Since recent reports [7–16,35] showed that exposure of prion proteins to low pH in endosomes was essential for the conversion from PrP^C to PrP^{Sc}, we tried to identify pH-sensitive regions by using the cysteine-scanning spin-labeling technique as described above. In the H1 region, we observed increases of $1/\delta H_0$ at E145R1, D146R1, and R147R1 when pH was decreased from 7.4 to 6.4 (Fig. 2). The values of R150R1 and E151R1 at pH 6.4 were similar to those at pH 7.4, but these values suddenly dropped when the pH in the solution changed from pH 6.4 to pH 5.0 as shown in Fig. 2B. In β-sheet regions of PrP, as shown in Fig. 3B, the mobility of S1 was conserved against a decrease of pH. However, the values of $1/\delta H_0$ at all four residues of S2 increased when pH was decreased from 6.4 to 5.0 (Fig. 4B). In particular, the region containing two N-terminal residues of S2, V160R1, and Y161R1 was identified as a more pH-sensitive region than that of C-terminal side residues of S2. Thus, the pH-sensitive domains, including the N-terminal tertiary contact site of H1 and the C-terminal ends of H1 and S2 regions, were identified in recombinant moPrP as shown in Fig. 5C. It is noteworthy that a slight decrease from pH 7.4 to 6.4 induced conformational changes in the N-terminal tertiary contact residues of H1 (E145R1, D146R1, and R147R1) though conformational changes in the C-terminal end of H1 (R150R1 and E151R1) and N-terminal residues of S2 (V160R1 and Y161R1) required a large change from pH 7.4 to 5.0. These findings led us to speculate that the conformational change from the tertiary contact structure to a more flexible structure in N-terminal residues of H1 was the first step for unfolding of PrP, followed by secondary conformational changes of S2 and the C-terminal end of H1.

In a previous NMR study of the globular domain (121–231) of hPrP [16], two domains, the C-terminal ends of the H1 and S2 regions, were identified as the pH-sensitive regions for acid-induced unfolding leading to a β-sheet rich structure. In addition to these two sites, the present SDSL–ESR study clearly demonstrated that the N-terminal region (E145, D146, and R147) of H1 was also a pH-sensitive region. The N-terminal tertiary contact region of H1 may be important for conversion from PrP^C to PrP^{Sc} in acidic conditions, since the structural change in this region easily occurred in a mildly acidic condition (pH 6.4) in comparison with the other two pH-sensitive regions. According to recent studies using MD simulations for PrP, histidine at 186 and asparagic acid at 177 of PrP were reported to be candidates for the amino acid residues that trigger the conversion to β-sheet-rich PrP [38,40]. This conversion model was based on the 3D structural changes due to disruption of a salt bridge with protonation of their amino acid residues caused by a decrease of pH. It is unclear whether these amino-acid residues were actually associated with pH-dependent conformational changes in H1 and S2 as observed in the present study. Further experiments to clarify this are now in progress.

In summary, the present cysteine-scanning SDSL–ESR study for H1, S1, and S2 of moPrP provided experimental evidence for three pH-sensitive sites, (1) the N-terminal tertiary contact site of H1, (2) the C-terminal end of H1, and (3) the S2 region. In particular, the present identification is the first report on a conformational change in the N-terminal tertiary contact site of H1 induced by mildly acidic conditions. This conformational change may be the first step in conversion of PrP^C to the pathogenic PrP^{Sc} structure in intracellular acidic organelles.

Acknowledgments

This work was supported, in part, by Grants-in-Aid for Basic Scientific Research from the Ministry of Education, Culture, Sports, Science and Technology of Japan (No. 17380178 and No. 18658118 [O.I.] and No. 17580275 and No. 17658126 [M.K.]), by Research Grants from the Program for the Center of Excellence of Zoonosis Control, Sapporo 060-0818, Japan [Y.W., O.I., M.H.], and CREST-JST, Multi-Quantum Coherence ESR Project, Muroran 050-8585, Japan [Y.S.].

References

[1] S.B. Prusiner, Prions, Proc. Natl. Acad. Sci. USA 95 (1998) 13363–13383.
[2] C. Weissmann, The Ninth Datta Lecture. Molecular biology of transmissible spongi form encephalopathies, FEBS Lett. 389 (1996) 3–11.
[3] S.B. Prusiner, Molecular biology of prion diseases, Science 252 (1991) 1515–1522.
[4] J.S. Griffith, Self-replication and scrapie, Nature 215 (1967) 1043–1044.
[5] C. Weissmann, Molecular genetics of transmissible spongiform encephalopathies, J. Biol. Chem. 274 (1999) 3–6.
[6] A. Aguzzi, M. Glatzel, F. Montrasio, M. Prinz, F.L. Heppner, Interventional strategies against prion diseases, Nat. Rev. Neurosci. 2 (2001) 745–749.
[7] S. Hornemann, R. Glockshuber, A scrapie-like unfolding intermediate of the prion protein domain PrP (121–231) induced by acidic pH, Proc. Natl. Acad. Sci. USA 95 (1998) 6010–6014.
[8] J.W. Kelly, The environmental dependency of protein folding best explains prion and amyloid diseases, Proc. Natl. Acad. Sci. USA 95 (1998) 930–932.
[9] W. Swietnicki, M. Morillas, S.G. Chen, P. Gambetti, W.K. Surewicz, Aggregation and fibrillization of the recombinant human prion protein huPrP (90—231), Biochemistry 39 (2000) 424–431.

[10] W. Swietnicki, R. Petersen, P. Gambetti, W.K. Surewicz, pH-dependent stability and conformation of the recombinant human prion protein PrP(90-231), J. Biol. Chem. 272 (1997) 27517–27520.
[11] G.S. Jackson, A.F. Hill, C. Joseph, L. Hosszu, A. Power, J.P. Waltho, A.R. Clarke, J. Collinge, Multiple folding pathways for heterologously expressed human prion protein, Biochim. Biophys. Acta. 1431 (1999) 1–13.
[12] Y. Matsunaga, D. Peretz, A. Williamson, D. Burton, I. Mehlhorn, D. Groth, F.E. Cohen, S.B. Prusiner, M.A. Baldwin, Cryptic epitopes in N-terminally truncated prion protein are exposed in the full-length molecule: dependence of conformation on pH, Proteins 44 (2001) 110–118.
[13] R. Zahn, The octapeptide repeats in mammalian prion protein constitute a pH-dependent folding and aggregation site, J. Mol. Biol. 334 (2003) 477–488.
[14] D.O. Alonso, S.J. DeArmond, F.E. Cohen, V. Daggett, Mapping the early steps in the pH-induced conformational conversion of the prion protein, Proc. Natl. Acad. Sci. USA 98 (2001) 2985–2989.
[15] D.O. Alonso, C. An, V. Daggett, Simulations of biomolecules: characterization of the early steps in the pH-induced conformational conversion of the hamster, bovine and human forms of the prion protein, Philos. Transact. A Math. Phys. Eng. Sci. 2002 (2002) 1165–1178.
[16] L. Calzolai, R. Zahn, Influence of pH on NMR structure and stability of the human prion protein globular domain, J. Biol. Chem. 278 (2003) 35592–35596.
[17] W.L. Hubbell, H.S. Mchaourab, C. Altenbach, M.A. Lietzow, Watching proteins move using site-directed spin labeling, Structure 4 (1996) 779–783.
[18] W.L. Hubbell, D.S. Cafiso, C. Altenbach, Identifying conformational changes with site-directed spin labeling, Nat. Struct. Biol. 7 (2000) 735–739.
[19] K.J. Oh, H. Zhan, C. Cui, K. Hideg, R.J. Collier, W.L. Hubbell, Organization of diphtheria toxin T domain in bilayers: a site-directed spin labeling study, Science 273 (1996) 810–812.
[20] L. Columbus, W.L. Hubbell, A new spin on protein dynamics, Trends Biochem. Sci. 27 (2002) 288–295.
[21] S. Mehboob, B.-H. Luo, W. Fu, M.E. Johnson, L.W.-M. Fung, Conformational studies of the tetramerization site of human erythroid spectrin by cysteine-scanning spin-labeling EPR methods, Biochemistry 44 (2005) 15898–15905.
[22] O. Inanami, S. Hashida, D. Iizuka, M. Horiuchi, W. Hiraoka, Y. Shimoyama, H. Nakamura, F. Inagaki, M. Kuwabara, Conformational change in full-length mouse prion: a site-directed spin-labeling study, Biochem. Biophys. Res. Commun. 335 (2005) 785–792.
[23] C.L. Kim, A. Umetani, T. Matsui, N. Ishiguro, M. Shinagawa, M. Horiuchi, Antigenic characterization of an abnormal isoform of prion protein using a new diverse panel of monoclonal antibodies, Virology 320 (2004) 40–51.
[24] Y. Imai, Y. Mastushima, T. Sugimura, M. Terada, A simple and rapid method for generating a deletion by PCR, Nucleic Acid Res. 19 (1991) 2785.
[25] O.H. Lowry, N.J. Rosebrough, A.L. Farr, R.J. Randall, Protein measurement with the Folin phenol reagent, J. Biol. Chem. 193 (1951) 265–275.
[26] N.R. Maiti, W.K. Surewicz, The role of disulfide bridge in the folding and stability of the recombinant human prion protein, J. Biol. Chem. 276 (2001) 2427–2431.
[27] R. Zahn, A. Liu, T. Lührs, R. Riek, C. Schroetter, F.L. García, M. Billeter, L. Calzolai, G. Wider, K. Wüthrich, NMR solution structure of the human prion protein, Proc. Natl. Acad. Sci. USA 97 (2000) 145–150.
[28] S. Hornemann, C. Korth, B. Oesch, R. Rieka, G. Widera, K. Wüthrich, R. Glockshubera, Recombinant full-length murine prion protein, mPrP (23–231): purification and spectroscopic characterization, FEBS Lett. 413 (1997) 277–281.
[29] D.G. Donne, J.H. Viles, D. Groth, I. Mehlhorn, T.L. James, F.E. Cohen, S.B. Prusiner, P.E. Wright, H.J. Dyson, Structure of the recombinant full-length hamster prion protein PrP (29–231): The N terminus is highly flexible, Proc. Natl. Acad. Sci. USA 94 (1997) 13452–13457.
[30] R. Riek, G. Wider, M. Billeter, S. Hornemann, R. Glockshuber, K. Wüthrich, Prion protein NMR structure and familial human spongiform encephalopathies, Proc. Natl. Acad. Sci. USA 95 (1998) 11667–11672.
[31] M. Vey, S. Pilkuhn, H. Wille, R. Nixon, S.J. DeArmond, E.J. Smart, R.G. Anderson, A. Taraboulos, S.B. Prusiner, Subcellular colocalization of the cellular and scrapie prion proteins in caveolae-like membranous domains, Proc. Natl. Acad. Sci. USA 93 (1996) 14945–14949.
[32] R.J. Lee, S. Wang, P.S. Low, Measurement of endosome pH following folate receptor-mediated endocytosis, Biochim. Biophys. Acta 1312 (1996) 237–242.
[33] G.H. Sun-Wada, Y. Wada, M. Futai, Vascuolar H^+ pumping ATPase in luminal acidic organelles and extracellular compartments: common rotational mechanism and diverse physiological roles, J. Bioenerg. Biomembr. 35 (2003) 347–358.
[34] G.H. Sun-Wada, Y. Wada, M. Futai, Lysosome and lysosome-related organelles responsible for specialized functions in higher organisms, with special emphasis on vacuolar-type proton ATPase, Cell Struct. Funct. 28 (2003) 455–463.
[35] M.L. DeMarco, V. Daggett, Local environmental effects on the structure of the prion protein, C. R. Biol. 28 (2005) 847–862.
[36] W.-Q. Zou, N.R. Cashman, Acidic pH and detergents enhance *in vitro* conversion of human, brain PrP^C to a PrP^{Sc} -like form, J. Biol. Chem. 277 (2002) 43942–43947.
[37] D.A. Kocisko, S.A. Priola, G.J. Raymond, B. Chesebro, P.T. Lansbury Jr., B. Caughey, Species specificity in the cell-free conversion of prion protein to protease-resistant forms: a model for the scrapie species barrier, Proc. Natl. Acad. Sci. USA 92 (1995) 3923–3927.
[38] E. Langella, R. Improta, V. Barone, Checking the pH-induced conformational transition of prion protein by molecular dynamics simulations: effect of protonation of histidine residues, Biophys. J. 87 (2004) 3623–3632.
[39] G.E. Pake, T.L. Estle, The Physical Principles of Electron Paramagnetic Resonance, second ed., Benjamin Inc., Reading, 1973 (Chapt. 6).
[40] J. Gsponer, P. Ferrara, A. Caflisch, Flexibility of the murine prion protein and its Asp178Asn mutant investigated by molecular dynamics simulations, J. Mol. Graph. Model 20 (2001) 169–182.

Jpn. J. Vet. Res. 53 (3 − 4) : 149-157, 2006

FULL PAPER

Alymphoplasia mice are resistant to prion infection via oral route.

Motohiro Horiuchi[1], Hidefumi Furuoka[2], Nobuo Kitamura[3] and Morikazu Shinagawa[4]

(Accepted for publication : February 14, 2006)

Abstract

The major cause of infection in animal prion diseases is thought to be consumption of prion-contaminated stuff. There is evidence that the enteric nerve system (ENS) and gut-associated lymphoid tissues (GATL) are involved in the establishment of prion infection through alimentary tract. To elucidate the initial entry port for prion, we inoculated prion to alymphoplasia (*aly*) mice showing a deficiency in systemic lymph nodes and Peyer's patches. The *aly/aly* mice were susceptible to prion infection by intra-cranial inoculation and there were no differences in incubation periods between *aly/aly* mice and wild-type C57BL/6J mice. Incubation periods in *aly/aly* mice were about 20 days longer than those in C57BL/6J mice with the intra-peritoneal inoculation. The *aly/aly* mice were completely resistant to prion infection by per os administration, while C57BL/6J mice were sensitive as they entered the terminal stage of disease around 300 days post inoculation. PrP^{Sc} were detected in the intestine and spleen of C57BL/6J mice inoculated with prion intraperitoneally or orally ; however PrP^{Sc} was not detected in the spleen and intestine of *aly/aly* mice. Prion infectivity was detected in the intestines and spleens of prion-inoculated C57BL/6J mice, even after the early stages of exposure, while no infectivity was detected in these tissues of prion-inoculated *aly/aly* mice. No apparent differences were observed in the organization of the enteric nerve system between wild-type and *aly/aly* mice. These results indicate that GALT rather than ENS acts as the primary entry port for prion after oral exposure.

[1]Laboratory of Prion Diseases, Graduate School of Veterinary Medicine, Hokkaido University, Sapporo 060-0818, Japan, [2]Laboratories of Veterinary Pathology and [3]Veterinary Anatomy, Obihiro University of Agriculture and Veterinary Medicine, Obihiro 080-8555, Japan, [4]Prion Disease Research Center, National Institute of Animal Health, Tsukuba 305-0856, Japan
Correspondence to : Motohiro Horiuchi, D.V.M., Ph. D.
Laboratory of Prion Diseases, Graduate School of Veterinary Medicine, Hokkaido University Kita-18 Nishi-9, Kita-ku, Sapporo 060-0818 Japan
Phone/Fax : +81-11-706-5293
e-mail : horiuchi@vetmed.hokudai.ac.jp

Key words : prion, scrapie, alymphoplasia, GALT

Introduction

Transmissible spongiform encephalopathies (TSEs or prion diseases) are a group of fatal neurodegenerative diseases that include scrapie in sheep and goats, bovine spongiform encephalopathy (BSE) in cattle, chronic wasting diseases (CWD) in deer and elk, and Creutzfeldt-Jakob disease in humans. Prion diseases have a long asymptomatic incubation period followed by a relatively short clinical phase, and they are characterized by the accumulation of disease-specific, protease-resistant isoforms of prion protein (PrP), designated PrP-res or PrP^{Sc}, in the central nervous system (CNS). PrP^{Sc} is post-translationally generated from the normal, protease-sensitive isoform of PrP, designated PrP-sen or PrP^{C}, which is expressed in many tissues and is particularly strongly expressed in the CNS. Although PrP^{Sc} is derived from host gene-encoded normal host protein, PrP^{C}, a line of evidences suggests that PrP^{Sc} is a major component of the TSE agent.

Although the CNS is the only site of histopathologically discernible damage, the port of entry for exogenous prion in animal prion diseases such as scrapie, BSE, and CWD is thought to be an alimentary tract. The route of neuroinvasion of prion has been well documented using prion-infected rodent models ; there are at least two pathways for neuroinvasion, one is retrograde along the parasympathetic fibers of the vagus nerve to the medulla oblongata, and the other is along the sympathetic fibers of the splanchnic nerve to the thoracic/lumbar spinal cord.[1-4] The existence of the two pathways to CNS is also confirmed by the extensive immunohistochemical analysis of naturally occurring sheep scrapie.[5] In the early stages of oral exposure to prion, PrP^{Sc} can be detected in the nerve cells of enteric nerve system (ENS) and follicular dendritic cells (FDC) of tonsil and other submucosal lymphoid follicules in the alimentary tract.[6-8] These data indicate that ENS and Gut-associated lymphoid tissues (GALT) are the initial entry port for prion infection. However, it is unclear which of these is primarily important for the establishment of prion infection in the alimentary tract and subsequent neuroinvasion..

The alymphoplasia (*aly*) mutation in mice is autosomal recessive and is characterized by a deficiency in systemic lymph nodes and Peyer's patches.[9] Recently, the *aly* allele was found to carry a point mutation causing in amino acid substitution in the carboxy-terminal of NF-κB inducing kinase (NIK).[10] Due to the lack of Peyer's patches, *aly* mice provide a suitable model for analyzing the involvement of GALT in the initial entry of prion in the alimentary tract. To elucidate the involvment of ENS and GALT in the establishment of prion infection, we analyzed the prion susceptibility of *aly* mice with various routes of infection. The results indicate GALT is a key tissue for the establishment of prion infection through the oral route.

Materials and Methods

Mice

ALY/NscJcl-*aly* (*aly*/*aly*) mice and their wild-type, C57BL/6J mice, were purchased from CLEA Japan Inc. ICR mice for bioassay were also purchased from CLEA Japan Inc.

Experimental inoculation

Mouse-adapted scrapie Obihiro strain was propagated in ICR mice. After entering the terminal stage of the disease, mice were sacrificed under anesthesia and brains were

collected. The brains were used as a source of brain homogenate for experimental inoculation. For intra-cranial (i.c.) inoculation, 20 μl of 1 % brain homogenate was injected into the left hemisphere. Mice assigned to the intraperitoneal (i.p.) inoculation group received 100 μl of 0.1% brain homogenate. Oral administration (p.o.) was carried out as described by Maignien et al.[11] Animals were placed in individual cages equipped with a liquid delivery system consisting of a 1.5-ml Eppendorf tube with a 3-mm hole at the bottom. Tubes were filled with 100 μl of a mixture of Endolipid (20% soya oil, 1.2% egg lecithin, 2.5% glycerol in water) and 20% brain homogenate (Endolipid : brain homogenate =1:1). Consumption of the infectious preparations was individually monitored.

Bioassay

During the course of experimental infection, 2 mice were sacrificed at each time point, and their brains, spleens and intestines were collected. Fifty milligrams of each tissue from the two mice was pooled and homogenized in PBS (10% w/w) a Multi-beads shocker (Yasuikiki, Japan) at 2,000 rpm for 1 min, followed by sonication for 30 sec. ICR mice were inoculated by i.c. route with 20 μl of the tissue homogenates and were observed until they exhibited the clinical symptoms of the terminal stage.

Detection of PrP^{Sc}

Samples were prepared as described previously,[12] with minor modifications described below. Minced tissues were homogenized in about eight volumes of buffer consisting of 2 % (v/v) Zwittergent 3-12, 0.5% sodium deoxycholate, 100 mM NaCl, and 50 mM Tris-HCl (pH7.5). Homogenates were digested with collagenase (0.5mg/100mg tissue) and DNase I (40μg/100mg tissue) with constant rotation at 37℃ for 6 to 12 hr until lumps of tissue were dispersed. Proteinase K (50 μg/100 mg tissue) was then added, and the homogenates were further incubated for 1 hr. Pefabloc was added at a final concentration of 2 mM to stop proteinase K digestion. Samples were then centrifuged at 68,000 g for 40 min at 20℃. The pellets were then dissolved in eight volumes (relative to the starting tissue sample) of 6.25% Sarkosyl in Tris-HCl, pH 8.0. After incubation at 37℃ for 30 min, the samples were centrifuged at 12,000g for 5 min at 20℃. Supernatants were a brought to 12% (w/v) NaCl, and were centrifuged at 100,000g for 40 min at 4 ℃. The resulting pellets were dissolved in sodium dodecyl sulfate-polyacrylaminde gel electrophoresis (SDS-PAGE) sample buffer (5% SDS, 4M Urea, 5% 2-mercaptoethanol, 10% glycerol, 0.02% bromophenol blue, 62.5 mM Tris-HCl, pH 6.8). Immunoblot was performed as described elsewhere with some modifications.[13] SDS-PAGE was carried out using 14% Bis-Tris gels (Invitrogen) according to the supplier's instruction. Western transfer to Immobilon-P transfer membranes (Millipore) was carried out using the Trans-blot mini cell (Bio-Rad) at 60 V for 2 hr. After transfer, membranes were blocked for 1 hr at room temperature with 5% skim milk in phosphate-buffered saline (PBS) containing0.1% Tween 20 (PBST) and were then incubated for 1 hr with primary antibodies diluted in the 1% skim milk in PBST. Blots were then washed with PBST and incubated with secondary antibody for 1 hr. Blots were visualized using an ECL Western blot detection kit (Amersham).

Immunochistochemical (IHC) detection of PrP^{Sc} was carried out as described elsewhere.[14] B103 polyclonal antibodies against bovine PrP synthetic peptide were used for detection.[15]

Staining of ENS

Tissues were fixed with 10% formalin, 0.2% picric acid in PBS, and wholemount specimens or cryosections (20 μm) were stained with antibodies against Protein Gene Product 9.5. Antibody reactivity of the antibody was visualized using the avidin-biotin complex method as described elsewhere.[16]

Results

Susceptibility of aly/aly mice to prion via various route of inoculation

In order to examine the susceptibility of *aly/aly* mice to prion infection, we inoculated *aly/aly* and C57BL/6J mice with brain homogenates of scrapie-infected mice via i.c., i.p. or p.o. route. Table 1 shows the incubation periods to reach the terminal stage of disease. No significant differences were observed in the incubation periods between *aly/aly* mice (159 days) and C57BL/6J mice (165 days) when they were inoculated with prion via i.c. route, and no apparent differences in clinical manifestation were seen between aly/aly and C57BL/6J mice. Furthermore, no differences were observed in the accumulation of PrP^{Sc} in the mouse brains (Fig. 1) or in neurohistopathological findings (data not shown), indicating that the *aly* phenotype, which is caused by a point mutation in NIK, dose not influence the neuropathogenesis of prion diseases nor prion replication in the CNS.

In i.p. inoculation, the incubation period in *aly/aly* mice was prolonged by 28 days, as

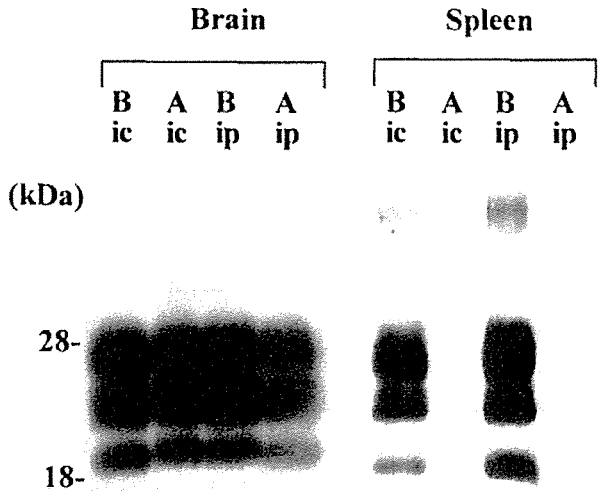

Fig. 1. Detection of PrP^{Sc} in brain and spleen. Mice exhibiting symptoms of the terminal stage of disease were sacrificed and examined for PrP^{Sc}. B, C57BL/6J mice; A, *aly/aly* mice. i.c., inoculated by intra-cranial route; i.p., inoculated by intra-peritoneal route. Molecular mass markers are in kilo Daltons.

compared with C57BL/6J mice, but all mice developed the typical clinical symptoms of scrapie. Although PrP^{Sc} levels in the brain were the same, there was a striking difference in the accumulation of PrP^{Sc} in spleen; PrP^{Sc} was not detected in the spleens of scrapie-affected *aly/aly* mice (Fig. 1). The severe combined immunodeficiency (SCID) mouse spleen did not support prion replication due to the lack of mature FDC, and SCID mice were found to be resistant to prion when low doses of prion were administered i.p. In contrast, SCID mice developed clinical symptoms with-

Table 1. Susceptibility of aly/aly mice to prion exposure via various routes.

Route	Concentration, amount of homogenate	Infectious dose[1] (LD_{50})	Period to terminal stage (days, mean ± SD)	
			C57BL/6J (Attack rate)	*aly/aly* (Attack rate)
i.c.	10%, 20 μl	10^6	165±5 (4/4)	159±8 (4/4)
i.p.	0.1%, 200 μl	10^5	251±9 (6/6)	279±6 (4/4)
p.o.	10%, 100 μl	5×10^6	307±7 (7/7)	>700 (0/5)

[1]Infectious doses were expressed as 50% lethal dose (LD_{50}).

out any PrP accumulation in the spleen when moderate doses of prion were administered i.p., although the incubation periods were longer than in wild-type mice.[17,18] This difference can be explained by direct spreading to the CNS from peripheral nerves. The prolonged incubation periods in *aly/aly* mice inoculated with prion via i.p route, without accumulation of PrP^{Sc} in spleen, could thus be explained by the same mechanism.

Obvious differences in susceptibility were observed when mice were challenged by p.o. route ; all of wild-type mice entered the terminal stage within 307 ± 7 days post infection (dpi) ; however, none of the *aly/aly* mice showed clinical symptoms and remained healthy throughout the experimental period (700 days). IHC analysis showed that PrP^{Sc} was present in the GATL of C57BL/6J mice at the terminal stage of the disease but was not present in that of *aly/aly* mice at the end of the experiment (Fig. 2). These results indicate that *aly/aly* mice are susceptible to prion replication in the CNS, but that neuroinvasion did not take place via oral consumption.

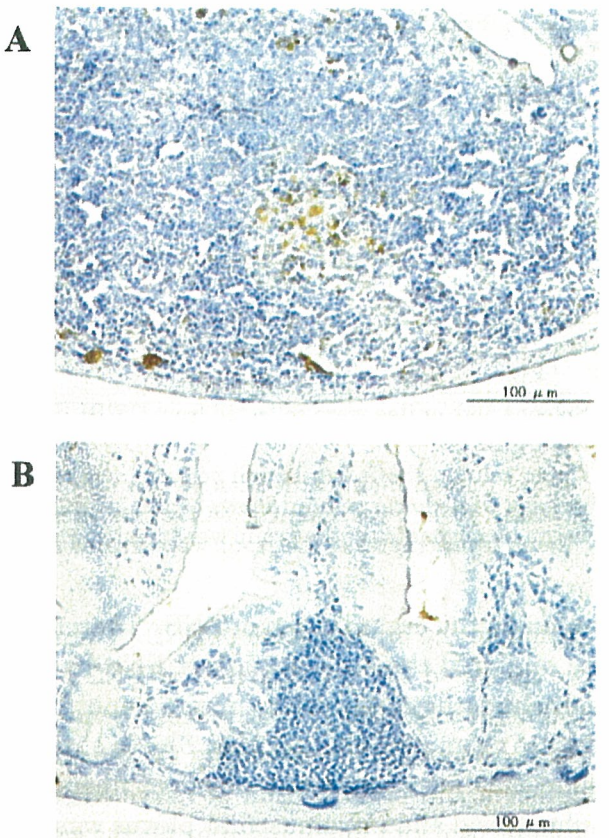

Fig. 2. Immunohistochemical detection of PrP^{Sc} in the ileum.
The ilea of mice inoculated p.o. were examined for PrP^{Sc}. (A) C5BL/6J mice at 309 dpi. (B) *aly/aly* mice at 700 dpi.

Prion infectivity in alimentary tract and spleen

In an effort to determine whether uptake and replication of prion occur in the alimentary tract of *aly/aly* mice, prion infectivity in the intestine was analyzed by bioassay. In the p.o. group, two mice from each mouse strain were sacrificed at 19, 43, and 83 dpi and tissue homogenates were inoculated i.c. into ICR mice for bioassay. Infectivity was detected in the intestines of C57BL/6J mice at each time point, however, no infectivity was detected in the intestines of *aly/aly* mice (Table 2), suggesting that prion did not replicate in the intestine of *aly/aly* mice. Infectivity was not detected in the spleens of *aly/aly* mice inoculated p.o., while considerable amounts of infectivity were detected in the spleens of the corresponding C57BL/6J mice at 80 dpi. Furthermore, traces of infectivity were detected in the spleens of *aly/aly* mice, even after i.p. inoculation ; one of five mice manifested the terminal stage of the disease at 381 dpi (Table 2) and the brain of this mouse was positive for PrP^{Sc} (data not shown), indicating that the lymphoid tissues of *aly/aly* mice did not support prion propagation.

Organization of ENS in aly/aly mice

Data described above suggested that GALT is essential as an initial entry port for prion infection, however, no information was available regarding the influence of NIK mu-

Table 2. Prion infectivity in spleen and ileum.

Group	dpi[1]	C57BL/6J		*aly/aly*	
		Spleen	Ileum	Spleen	Ileum
p.o.	19	NT[2]	246±36 (6/6)[3] 6.3×10^3	NT	>300 (0/5)
	43	NT	220±18 (4/4) 3.7×10^4	NT	>425 (0/5)
	83	176±4 (5/5) 8.9×10^6	307±21 (5/5)[4] 6.2×10^2	>450 (0/5)	>450 (0/5)[4]
i.p.	80	188±31 (4/4) 2.0×10^6	NT	>450 (0/4) 381 (1/5)	NT

[1]Spleens and/or ilea were collected from C57BL/6J or *aly/aly* mice at indicated days post infection.
[2]Not tested.
[3]Upper column shows incubation periods (days, mean ± SD) and attack rates (in parenthesis) of mice used for bioassay, while lower column shows estimated infectivity (LD_{50}/g tissue) from the incubation periods.
[4]Ileum homogenates of the group were treated at 60℃ for 30 min before inoculation to mice for bioassay.

tation on the organization of ENS. Therefore, we analyzed the organization of ENS by immunohistochemistry with protein gene product 9.5 as an ENS marker (Fig. 3). No obvious deficiency in organization of nerve fibers, or submucosal and intramuscular plexus was observed in *aly/aly* mice, supporting the idea that GALT is a primary target for prion entry via oral consumption.

Discussion

Although the pathway of invasion into CNS is well characterized,[1,3-5] it remains unclear how prion enter the host, particularly under natural circumstance. The major route of infection in naturally occurring prion diseases in animals is believed to be oral consumption of the infectious agent. Accumulating evidence suggests that the ENS and GALT are the primary target sites for prion entry and replication in peripheral tissues.[1,3,4] We therefore attempted to address the question of whether the ENS or GALT is important in the establishment of prion infection via the oral route. Our results demonstrated that GALT is essential for initial uptake of prion from the gut lumen to the alimentary tract. No differences were observed

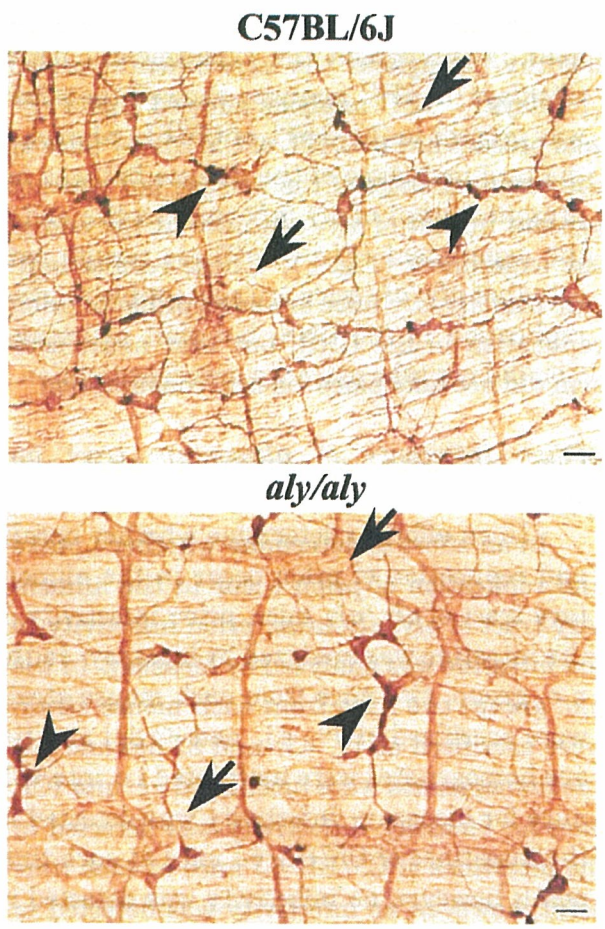

Fig. 3. Organization of enteric nerve system. Extended intestine specimens were stained with anti-protein gene product 9.5 antibodies. Arrowheads indicate submucosal plexus, whereas arrows indicate intra-muscular plexus. Bar : 50 μm

in the organization of ENS between *aly/aly* and C57BL/6J mice, suggesting that prion adsorption via the epithelial cells of digestive tract and subsequent entrance into peripheral nerve fibers or blood stream is unlikely.

The follicle-associated epithelium (FAE) that covers the dome of Peyer's patches or submucosal lymphoid follicle contains villus and M cells. M cells act as major ports of entry for enteric pathogens via trans epithelial transport[19], and Heppner *et al.* reported that prion could be transported from the apical to the basolateral compartment in an *in vitro* model comprising epithelial cells morphologically and functionally resembling M cells.[20] It was reported that functional B cells are required for the development of the FAE, Payer's patches and M cells.[21] B cells of *aly/aly* mice are functionally impaired so that *aly/aly* mice may have reduced M cell numbers and/or functionally impaired M cells in FAE. Mice deficient in B lymphocytes (μMT mice), both B and T lymphocytes (RAG-$1^{-/-}$ mice), or in tumor necrosis factor and lymphptoxin-α, in which the number of Peyer's patches is reduced, were resistant to oral prion challenge.[22] In contrast, β7 integrin-deficient mice, in which B cells in Peyer's patches are severely reduced, which also possess normal numbers of Peyer's patches, were sensitive to oral prion infection.[22] The difference in prion susceptibility among those B cell-deficient mice following oral inoculation may be explained by the numbers of Peyer's patches and M cells.[22] The *aly/aly* mice were highly resistant to oral prion infection, similar to RAG-$1^{-/-}$ and μMT mice, and thus it is of interest to determine whether the presence of M cells and M cell function in *aly/aly* mice are involved in the initial entry of prion into the gastro-intestinal tract.

One of the interesting questions is why ruminants appear sensitive to prion via oral exposure. Anatomical and histological characteristics might explain the susceptibility of ruminants to prion. The ileal Peyer's patches are large organs in young lambs, extending for up to 2.5 cm, are estimated to contain over 100,000 follicles,[23] and develop well in the distal ileum. FEA of cattle was reported to contain higher M cell or M cell-like populations than that of rodents.[23,24] These features suggest that the intestines of ruminant possess more ports of entry for prion than those of rodents. The scrapie susceptibility of sheep is thought to decline with growth.[25] The involution of the ileal Peyer's patch at puberty and the accompanying drastic reduction in the number of follicles and FAE may contribute to the reduced susceptibility to prion that is observed in older animals.

PrP^{Sc} and prion infectivity can be readily detected in the lymphoreticular tissues of scrapie-infected sheep, in contrast, PrP^{Sc} and prion infectivity were scarcely detected in the lymphoreticular tissues of BSE-affected cattle.[26] However, PrP^{Sc} has been detected in the ENS of BSE-affected cattle (Iwata et al., submitted for publication). Thus efficient replication of BSE agent in peripheral lymphoreticular tissues may not be essential for the neuroinvasion of BSE agent after oral exposure. The *aly/aly* mice possess normal ENS organization but are resistant to prion infection via the p.o. route, suggesting that the ENS does not act as a port of entry for prion after oral exposure.

Acknowledgements

This work was supported by a grant from The 21st Century COE Program (A-1) and a Grant-in-Aid for Science Research (A) (grant 15208029) from the Ministry of Education, Culture, Sports, Science, and Technology, Japan. This work was also supported by a grant from the Ministry of Health, Labour and Wel-

fare of Japan.

References

1) Muramoto, T., Kitamoto, T., Tateishi, J. and Goto, I. 1992. The sequential development of abnormal prion protein accumulation in mice with Creutzfeldt-Jakob disease. *Am. J. Pathol.*, 140 : 1411-1420.

2) Beekes, M., Baldauf, E. and Diringer, H. 1996. Sequential appearance and accumulation of pathognomonic markers in the central nervous system of hamsters orally infected with scrapie. *J. Gen. Virol.*, 77 : 1925-1934.

3) McBride, P. A., Schulz-Schaeffer, W. J., Donaldson, M., Bruce, M., Diringer, H., Kretzschmar, H. A. and Beekes, M. 2001. Early spread of scrapie from the gastrointestinal tract to the central nervous system involves autonomic fibers of the splanchnic and vagus nerves. *J. Virol.*, 75 : 9320-9327.

4) Mabbott, N. A. Bruce, M.E. 2001. The immunobiology of TSE diseases. *J. Gen. Virol.*, 82 : 2307-2718.

5) van Keulen, L. J., Schreuder, B. E., Vromans, M. E., Langeveld, J. P. and Smits, M. A. 2000. Pathogenesis of natural scrapie in sheep. *Arch. Virol., Suppl*. 16 : 57-71.

6) Beekes, M. and McBride, P. A. 2000. Early accumulation of pathological PrP in the enteric nervous system and gut-associated lymphoid tissue of hamsters orally infected with scrapie. *Neurosci. Lett.*, 278 : 181-184.

7) Andreoletti, O., Berthon, P., Marc, D., Sarradin, P., Grosclaude, J., van Keulen, L., Schelcher, F., Elsen, J-M. and Lantier, F. 2000. Early accumulation of PrP^{Sc} in gut-associated lympoid and nerous tissues of susceptible sheep from a romanov flock with natural scrapie. *J. Gen. Virol.*, 81 : 3115-3126.

8) Sigurdson, C. J., Spraker, T. R., Miller, M. W., Oesch, B.and Hoover, E. A. 2001. PrP^{CWD} in the myenteric plexus, vagosympathetic trunk and endocrine glands of deer with chronic wasting disease. *J. Gen. Virol.*, 82 : 2327-2334.

9) Miyawaki, S., Nakamura, Y., Suzuka, H., Koba, M., Yasumizu, R., Ikehara, S. and Shibata, Y. 1994. A new mutation, aly, that induces a generalized lack of lymph nodes accompanied by immunodeficiency in mice. *Eur. J. Immunol.*, 24 : 429-434.

10) Shinkura, R., Kitada, K., Matsuda, F., Tashiro, K., Ikuta, K., Suzuki, M., Kogishi, K., Serikawa, T. and Honjo, T. 1999. Alymphoplasia is caused by a point mutation in the mouse gene encoding Nf-kappa b-inducing kinase. *Nat. Genet.*, 22 : 74-77.

11) Maignien, T., Lasmezas, C. I., Beringue, V., Dormont, D. and Deslys, J. P. 1999. Pathogenesis of the oral route of infection of mice with scrapie and bovine spongiform encephalopathy agents. *J. Gen. Virol.*, 80 : 3035-3042.

12) Grathwohl, K.-U., Horiuchi, M., Ishiguro, N. and Shinagawa, M. 1996. Improvement of PrP^{Sc}-detection in mouse spleen early at the preclinical stage of scrapie with collagenase-completed tissue homogenization and Sarkosyl-NaCl extraction of PrP^{Sc}. *Arch. Virol.*, 141 : 1863-1874.

13) Kim, C.-L., Umetani, A., Matsui, T., Ishiguro, N., Shinagawa, M.and Horiuchi, M. 2004. Antigenic characterization of an abnormal isoform of prion protein using a new diverse panel of monoclonal antibodies. *Virology*, 320 : 40-51.

14) Furuoka, H., Yabuzoe, A., Horiuchi, M., Tagawa, Y., Yokoyama, T., Yamakawa, Y., Shinagawa, M. and Sata, T. 2005. Effective antigen-retrieval method for immunohistochemical detection of abnormal

isoform of prion proteins in animals. *Acta Neuropathol.,* 109 : 263-271.

15) Horiuchi, M., Yamazaki, N., Ikeda ,T., Ishiguro, N. and Shinagawa, M. 1995. A cellular form of prion protein (PrPC) exists in many non-neuronal tissues of sheep. *J. Gen. Virol.,* 76 : 2583-2587.

16) Kitamura, N., Mori, Y., Hondo, E., Baltazar, E. T. and Yamada, J. 1999. An immunohistochemical survey of catecholamine-synthesizing enzyme-immunoreactive nerves and endocrine cells in the bovine pancreas. *Anat. Histol. Embryol.,* 28 : 81-84.

17) O'Rourke, K. I., Huff, T. P., Leathers, C. W., Robinson, M. M. and Gorham, J. R. 1994. SCID mouse spleen does not support scrapie agent replication. *J. Gen. Virol.,* 75 : 1511-1514.

18) Lasmezas, C. I., Cesbron, J. Y., Deslys, J. P., Demaimay, R., Adjou, K. T., Rioux, R., Lemaire, C., Locht, C. and Dormont ,D. 1996. Immune system-dependent and-independent replication of the scrapie agent. *J. Virol.,* 70 : 1292-1295.

19) Neutra, M. R., Frey, A. and Kraehenbuhl, J. P. 1996. Epithelial M cells : gateways for mucosal infection and immunization. *Cell,* 86 : 345-348.

20) Heppner, F. L., Christ, A. D., Klein, M. A., Prinz, M., Fried, M., Kraehenbuhl, J. P. and Aguzzi, A. 2001. Transepithelial prion transport by M cells. *Nat. Med.,* 7 : 976-977.

21) Golovkina, T. V., Shlomchik, M., Hannum, L. and Chervonsky, A. 1999. Organogenic role of B lymphocytes in mucosal immunity. *Science,* 286 : 1965-1968.

22) Prinz, M., Huber, G., Macpherson, A. J., Heppner, F. L., Glatzel, M., Eugster, H. P., Wagner, N. and Aguzzi, A. 2003. Oral prion infection requires normal numbers of Peyer's patches but not of enteric lymphocytes. *Am. J. Pathol.,* 162 : 1103-1111.

23) Reynolds, J. D. and Morris, B. 1983. The evolution and involution of Peyer's patches in fetal and postnatal sheep. *Eur. J. Immunol.,* 13 : 627-635.

24) Momotani, E., Whipple, D. L., Thiermann, A. B. and Cheville, N. F. 1988. Role of M cells and macrophages in the entrance of mycobacterium paratuberculosis into domes of ileal Peyer's patches in calves. *Vet. Pathol.,* 25 : 131-137.

25) Hourrigan, J. L., Klingsporn, A., Clark, W. W. and Decamp, M. 1979. Epidemiology of scrapie in the United States. In : *Slow transmissible diseases of the nervous system*, pp. 331-336, Prusiner, S. B. and Hadlow, W. J. ed., Acdemic Press, New York.

26) Wells, G. A., Spiropoulos, J., Hawkins, S. A. and Ryder, S. J. 2005. Pathogenesis of experimental bovine spongiform encephalopathy : preclinical infectivity in tonsil and observations on the distribution of lingual tonsil in slaughtered cattle. *Vet. Rec.,* 156 : 401-407.

FULL PAPER *Clinical Pathology*

Sequence Variation of Bovine Prion Protein Gene in Japanese Cattle (Holstein and Japanese Black)

Satoshi NAKAMITSU[1], Takayuki MIYAZAWA[1], Motohiro HORIUCHI[2], Sadao ONOE[3], Yasunori OHOBA[4], Hitoshi KITAGAWA[4] and Naotaka ISHIGURO[5]*

[1]*Laboratory of Veterinary Public Health, Obihiro University of Agriculture and Veterinary Medicine, Obihiro, Hokkaido 080–8555,* [2]*Laboratory of Prion Disease, Graduate School of Veterinary Medicine, Hokkaido University, Sapporo, Hokkaido 060–0813,* [3]*Molecular Biotechnology Laboratory, Hokkaido Animal Research Center, Shintoku, Hokkaido 081–0038,* [4]*Laboratories of Internal Medicine and* [5]*Food and Environmental Hygiene, Faculty of Applied Biological Science, Gifu University, Gifu 501–1193, Japan*

(Received 9 June 2005/Accepted 16 September 2005)

ABSTRACT. To assess relationships between nucleotide polymorphisms of the prion protein (*PRNP*) gene and susceptibility to bovine spongiform encephalopathy (BSE), we investigated polymorphisms in the open reading frame (ORF) and 2 upper regions of the *PRNP* gene from 2 Japanese cattle breeds: 863 healthy Holstein cattle, 6 BSE-affected Holstein cattle, and 186 healthy Japanese Black (JB) cattle. In the ORF, we found single-nucleotide polymorphisms (SNPs) at nucleotide positions 234 and 576 and found 5 or 6 copies of the octapeptide repeat, but we did not find any amino acid substitutions. In the upper region, we examined 2 sites of insertion/deletion (indel) polymorphisms: a 23-bp indel in the upper region of exon 1, and a 12-bp indel in the putative promoter region of intron 1. A previous report suggests that the 23-bp indel polymorphism is associated with susceptibility to BSE, but we did not find a difference in allele frequency between healthy and BSE-affected Holstein cattle. There were differences in allele frequency between healthy Holstein and JB cattle at the 23- and 12-bp indels and at the SNPs at nucleotide positions 234 and 576, but there was no difference in allele frequency of the octapeptide repeat. We identified a unique *PRNP* gene lacking a 288-bp segment (96 amino acids) in DNA samples stocked in our laboratory, but this deletion was not found in any of the 1049 cattle examined in the present study. The present results provide data about variations and distribution of the bovine *PRNP* gene.

KEY WORDS: BSE, cattle, polymorphism, prion, *PRNP*.

J. Vet. Med. Sci. 68(1): 27–33, 2006

Transmissible spongiform encephalopathies (TSEs) are a group of fatal neurodegenerative diseases that include Creutzfeldt-Jakob disease (CJD), Gerstmann-Sträussler-Scheinker syndrome (GSS), Kuru and fatal familial insomnia (FFI) in humans, scrapie in sheep and goats, chronic wasting disease (CWD) in deer and elk, feline spongiform encephalopathy (FSE) in cats, transmissible mink encephalopathy (TME) in minks, and bovine spongiform encephalopathy (BSE) in cattle [26,27]. The hallmarks of TSE are neuronal vacuolation, astrocytosis, and accumulation of a pathogenic, abnormal and protease-resistant isoform of prion protein (PrP), designated PrP^{Sc} or prion, in the central nervous system. PrP^{Sc} is generated from the endogenous cellular prion protein PrP^{C}, encoded by the prion protein gene (*PRNP*), by post-translational modification leading to conformational changes [26, 27]. It has been hypothesized that PrP^{C} plays a role in copper metabolism [20, 32], but the normal functions of PrP^{C} in cells are unclear.

It is generally believed that BSE epidemics in cattle are caused by ingestion of meat and bone meal contaminated with PrP^{Sc} [35]. BSE appears to pose a threat not only to cattle but also to human public health, because the human disease variant CJD (vCJD) is thought to be caused by ingestion of meat or meat products contaminated with BSE [3, 30]. Genetic resistance to TSE is thought to be an important factor in prevention of disease recurrence. In the open reading frame (ORF) of the *PRNP* gene, amino acid polymorphisms associated with prion disease susceptibility and incubation period have been found in humans [24], sheep [2, 4, 13] and mice [34]. Sheep with valine at codon 136 and glutamine at codon 171 ($V^{136}Q^{171}$ animals) exhibit high susceptibility and short incubation period for scrapie, whereas sheep with alanine at codon 136 and arginine at codon 171 ($A^{136}R^{171}$ animals) exhibit resistance to scrapie [2, 13]. An analysis of the ORF of the *PRNP* gene of cattle (*Bos Taurus*) revealed several nucleotide substitutions including an octapeptide repeat polymorphism, but it is unclear whether the polymorphisms correlate with BSE [6, 12,14, 23, 28].

In Japan, the first BSE-affected animal was found in September 2001, and a total of 20 BSE-infected cattle have been found at end of July, 2005. There have been few reports about sequence variations in the *PRNP* gene of Holstein and Japanese Black (JB) cattle, which are widely raised in Japan [31]. The purpose of the present study was to examine variations of the *PRNP* gene in Holstein and JB cattle in Japan, including estimation of the relationship between bovine *PRNP* polymorphisms and occurrence of BSE.

MATERIALS AND METHODS

Animals and DNA samples: We examined 1049 healthy cattle: 863 Holstein cattle from Hokkaido Prefecture in Japan (489 cattle from 8 dairy farms, and 374 cattle from a

* CORRESPONDENCE TO: ISHIGURO, N., Laboratory of Food and Environmental Hygiene, Faculty of Applied Biological Science, Gifu University, Gifu, 501–1193, Japan.

slaughterhouse), and 189 JB cattle from 5 districts in Gifu Prefecture. We also examined 6 BSE-affected Holstein cattle, from Hokkaido (3 cases), Gunma (1 case), Kanagawa (1 case) and Wakayama (1 case) Prefectures (http://www.mhlw.go.jp/topics/0103/tp0308-1.html). DNA was isolated from blood samples from healthy Holstein and JB cattle, and from meat or the medulla oblongata of BSE-affected cattle, using the QIAamp DNA Blood Mini Kit (Qiagen Science, Germantown, MD). Blood was also directly used for polymerase chain reaction (PCR) with an Ampdirect kit (Shimadzu biotech, Kyoto, Japan). The 52 DNA samples (15 samples from sporadic bovine leucosis, 6 samples from enzootic bovine leucosis, 5 samples from tumor, 16 samples from the other diseases and 10 samples from healthy cattle) stocked in our laboratory were examined in the present study.

DNA amplification: We examined 3 regions for nucleotide polymorphisms: a 23-bp indel polymorphism about 1.5 kb upstream of exon 1, a 12-bp indel polymorphism in intron 1, and the entire ORF of exon 3. To determine DNA sequences, 795 bp of the ORF of the bovine *PRNP* gene (nt 65579 to 66373 in accession number AJ298878 [9]) were amplified using the primers BPrP3 (5'GCAGATATAAGTCATCATGGTG) and BPrP4 (5'GAAGATAATGAAAACAGGAAGG), as described by Gombojav *et al.* [7] (Fig. 1). To assay the octapeptide (PHGGGWGQ) repeat and the 288-bp deletion in the ORF of the bovine *PRNP* gene, we directly amplified the N-terminal region (577 to 565 bp) of the ORF using 0.7 μl of blood (863 Holstein and 186 JB cattle) in 25 μl of Ampdirect buffer containing 1 unit of Taq polymerase (Sigma Aldrich, St. Louis, MO), 10 pmol of the primers BPrP3 and SP4 (5'CATTGGTCTTGTTGAAACAC) and 2 mM dNTPs, according to the Ampdirect kit instructions. To examine the 23-bp insertion/deletion (indel) polymorphism in the upper region of exon 1 (A, 23-bp indel in Fig. 1), we amplified 123 or 100 bp using the primers PRNP47784 and PRNP47883R and DNA specimens from 278 Holstein and 186 JB cattle [28]. For the 12-bp indel polymorphism in intron 1 of the bovine *PRNP* gene (B, 12-bp indel in Fig. 1), we amplified 414 or 426 bp using the primers BPrP30 (5'CTTCTCTCTCGCAGAAGCAG) and BPrP32 (5'CCCTTGTTCTTCTGAGCTCC) and DNA specimens from 290 Holstein and 186 JB cattle. The thermal cycling sequence of the amplification was as follows: initial denaturation at 94°C for 10 min; 50 cycles of denaturation at 94°C for 30 s, annealing at the annealing temperature of the specific primer pair for 30 s, and extension at 72°C for 1 min; final extension at 72°C for 7 min. All PCR products were electrophoresed to assess yield and purity on 1.5% to 3.0% agarose gels, and were then photographed. The PCR product for the 12-bp indel (414 or 426 bp) was digested with *Sac*II enzyme and separated on 2% agarose gel to assay for the presence of the 12-bp indel, because the 12-bp indel sequence contains a *Sac*II recognition site.

DNA sequencing: PCR products were purified using the QIAquick PCR Purification Kit (Qiagen) for DNA sequencing. Purified PCR products of the bovine *PRNP* gene were directly sequenced using internal sequencing primers SP1 (5'TTGGTGGCTACATGCTGGGAAG) and SP4. Sequencing was performed using an ABI 310 DNA sequencer with an ABI PRISM BigDye Terminator v3.1 Cycle Sequencing Kit. Alignment of sequences was performed using GENETYX-MAC software (Software Development Co., Tokyo, Japan).

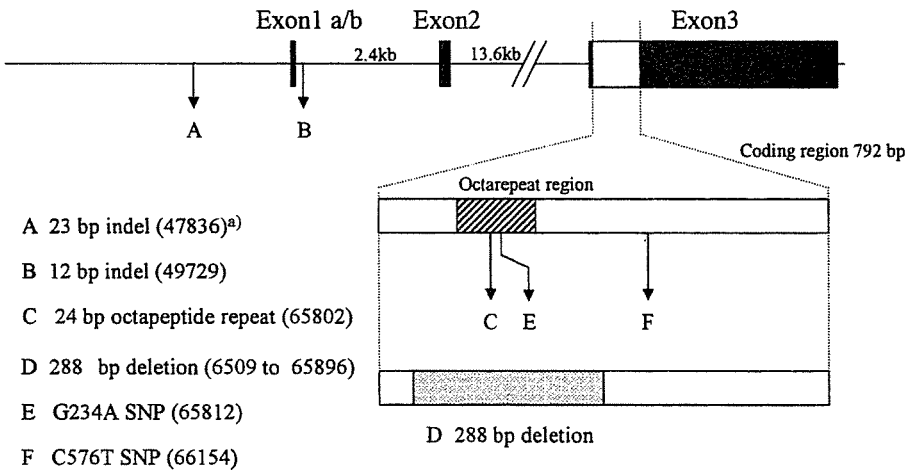

Fig. 1. Diagram of genomic structure of the bovine *PRNP* gene. The 6 polymorphisms (3 indels, 1 deletion and 2 SNPs) found in the present study are indicated by arrows labeled with letters. The 3 *PRNP* exons are represented by black boxes, and the protein-coding region in exon 3 is shown as a white area in the black box [11]. The hatched portion of the coding region indicates the octarepeat region. The dotted portion of the coding region indicates the 96-amino-acid (288-bp) deletion from nt 65609 to 65896 in reference sequence AJ298878 [9]. a) The numbers in parentheses indicate positions in reference sequence AJ298878.

Statistical analysis: We used the χ-square test to assess the significance of associations between allele distribution and BSE among Holstein and JB cattle.

RESULTS

Polymorphisms in the upstream region: Representative results for the 23-bp indel are shown in Fig. 2A. Cattle homozygous for the 23-bp deletion or insertion showed one distinct band, at 100 or 123 bp, respectively (Fig. 2A, designated by –/– and +/+). Cattle heterozygous for the 23-bp indel showed two bands: at 123 and 100 bp (Fig. 2A, +/–). The majority of the Holstein cattle tested for the 23-bp indel (62%) were homozygous for the 23-bp deletion, whereas the majority of the JB cattle (61%) were heterozygous for the 23-bp indel (Table 1). For cattle homozygous for the 12-bp insertion, the *Sac*II enzyme cleaved the PCR product (426 bp) into two fragments: 276 and 150 bp. Cattle homozygous for the 12-bp deletion showed a single band at 414 bp. Cattle heterozygous for the 12-bp indel showed three distinct bands: 414, 276 and 150 bp (Fig. 2B, +/–). Most of the Holstein cattle tested for the 12-bp indel were either heterozygous or were homozygous for the 12-bp deletion, but 61% of the JB cattle were heterozygous.

Among the 6 BSE-affected cattle, 2 cattle were heterozygous at both the 23- and 12-bp indels, and 4 cattle were homozygous at both the 23- and 12-bp indels.

Polymorphisms of ORF in PRNP: In the present study, we found a mutant with a 288-bp deletion (96 amino acids from codon 11 to codon 108) among 52 DNA samples stocked in our laboratory (Fig. 1). The N-terminal region amplified from the 288-bp-deletion mutant showed two bands: one band containing 6 copies of the octapeptide repeat (575 bp), and the other small band (287 bp) with the 288-bp deletion (Fig 2D). None of the 1049 cattle tested carried the 288-bp deletion in the *PRNP* gene. Among both Holstein and JB cattle, the predomininat genotype of the octapeptide repeat was homozygosity for the 6-copy allele (575 bp in Fig. 2C, designated as 6/6), followed by heterozygosity for 5 and 6 copies (Fig. 2C, 6/5) (Table 1). Only 4 Holstein cattle and none of the JB cattle were homozygous for 5 copies of the octapeptide repeat (Fig. 2C, 5/5). All BSE-affected cattle had 6 copies of the octapeptide repeat. We detected 2 single-nucleotide polymorphisms (SNPs) at G234A and C576T in 232 Holstein and 186 JB cattle (Table 1). At the C576T SNP, none of the Holstein cattle were homozygous for thymine, but 28 of the JB cattle were homozygous for thymine.

Statistical analysis of nucleotide polymorphisms: Allele frequencies of nucleotide polymorphisms at the 2 indels (23 and 12 bp), the octapeptide repeat and 2 SNPs (nt 234 and 576) are shown in Table 2. There was no significant difference between healthy and BSE-affected Holstein cattle at any of the nucleotide polymorphisms. At the 23- and 12-bp indels and the G234A and C576T SNPs, there were significant differences in allele frequency between healthy Holstein and JB cattle (Table 2).

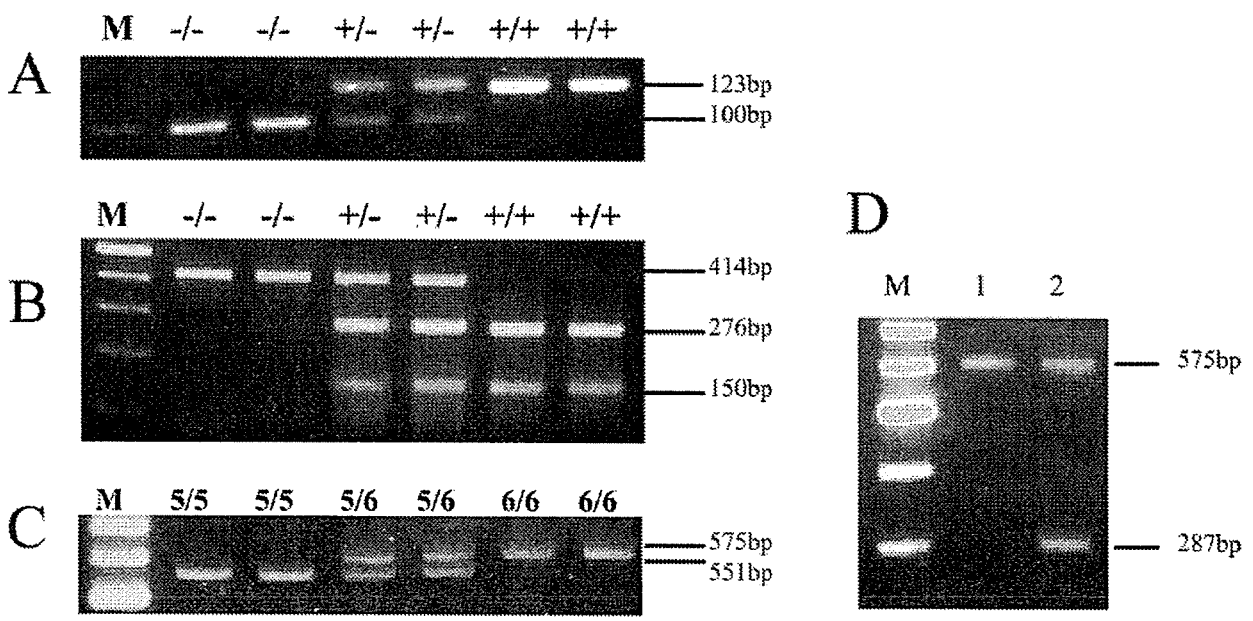

Fig. 2. Genotyping of insertion or deletion polymorphisms by agarose gel electrophoresis. A) Genotypes of 6 different cattle are indicated as presence (+) or absence (–) of 23-bp insertion. B) Genotypes of *Sac*II-digested PCR products from 6 different cattle are indicated as presence (+) or absence (–) of 12-bp insertion. C) Genotypes of octapeptide repeats (homozygote 5/5, heterozygote 5/6 and homozygote 6/6). D) Genotypes of N-terminal region of *PRNP* gene amplified using primers BPrP3 and SP4: lane 1, PCR product from 6/6 homozygote; lane 2, PCR product from 288-bp-deletion mutant. M, 100-bp DNA size marker.

Table 1. Genotype frequency of polymorphisms among healthy Holstein, healthy JB cattle and BSE-affected Holstein cattle

Breed and location		N[f]	23-bp indel[a]			12-bp indel[b]			Octarepeat[c]			G234A[d]			C576T[e]		
			+/+	+/–	–/–	+/+	+/–	–/–	6/6	6/5	5/5	G/G	G/A	A/A	C/C	C/T	T/T
Healthy Holstein	A	15	1	8	6	2	8	5	13	2	0	6	7	2	15	0	0
	B	27	3	12	11	4	16	6	23	4	0	17	7	3	27	0	0
	C	168	0	36	127	0	45	117	148	19	1	59	11	4	72	2	0
	D	74	10	34	30	11	37	26	61	13	0	–	–	–	–	–	–
	E	13	–	–	–	4	4	5	10	3	0	7	2	4	13	0	0
	F	51	–	–	–	–	–	–	47	4	0	32	10	9	51	0	0
	G	125	–	–	–	–	–	–	109	14	2	43	9	0	52	0	0
	H	16	–	–	–	–	–	–	14	2	0	–	–	–	–	–	–
	I	374	–	–	–	–	–	–	340	33	1	–	–	–	–	–	–
Total healthy Holstein		863	14	90	174	21	110	159	765	94	4	164	46	22	230	2	0
Healthy JB[g]																	
	J	37	3	29	5	3	26	8	37	0	0	6	25	6	13	20	4
	K	37	7	24	6	10	22	5	30	7	0	11	19	7	18	14	5
	L	31	0	11	20	0	13	18	28	3	0	16	15	0	4	16	11
	M	40	4	22	14	6	24	10	37	3	0	13	21	6	17	20	3
	N	41	5	28	8	5	28	8	41	0	0	10	27	4	15	21	5
Total healthy JB		186	19	114	53	24	113	49	173	13	0	56	107	23	67	91	28
Total healthy Holstein and healthy JB		1049	33	204	227	45	223	208	938	107	4	220	153	45	297	93	28
BSE-affected Holstein		6	0	2	4	0	2	4	6	0	0	4	1	1	6	0	0

a) The 23-bp indel polymorphism in the upper region of exon 1 in Fig.1.
b) The 12-bp indel polymorphism in intron 1 in Fig.1.
c) Octarepeat polymorphism of the coding region.
d),e) Polymorphism at nt 234 and 576 in the ORF, respectively.
f) Number of samples collected.
g) JB, Japanese Black.

Table 2. Allele frequency of nucleotide polymorphisms among healthy Holstein, healthy JB cattle and BSE-affected Holstein cattle

Breed	Nucleotide polymorphisms																			
	23-bp insertion				12-bp insertion				Octarepeat[c]				G234A				C576T			
	n[a]	+[b]	–[c]	p[d]	n	+	–	p	n	6	5	p	n	G	A	p	n	C	T	p
Healthy Holstein	278	0.21	0.79		290	0.26	0.74		863	0.94	0.06		232	0.81	0.19		232	1.00	0	
BSE Holstein	6	0.17	0.83	n.s[f]	6	0.17	0.83	n.s	6	1.00	0	n.s	6	0.75	0.25	n.s	6	1.00	0	n.s
Subtotal	284	0.21	0.79		296	0.27	0.74		869	0.94	0.06		238	0.80	0.20		238	1.00	0	
Healthy JB	186	0.41	0.59	<0.01	186	0.43	0.57	<0.01	186	0.97	0.03	n.s	186	0.56	0.41	<0.01	186	0.60	0.40	<0.01
Healthy JB and Holstein	464	0.29	0.71		476	0.33	0.67		1049	0.95	0.05		418	0.71	0.29		418	0.82	0.18	

a) n, number of cattle examined.
b) +, 23-bp or 12-bp insertion.
c) –, 23-bp or 12-bp deletion.
d) $p<0.01$, significant difference among the compared values.
e) Five or 6 copies of octapeptide repeat.
f) n.s, not significant.

DISCUSSION

PRNP polymorphisms are associated with variation in susceptibility to prion disease in humans [24], sheep [2, 4, 5, 13] and mice [34]. There have been many studies of relationships between *PRNP* polymorphisms and susceptibility to BSE in cattle [8, 12, 14, 22, 25, 28, 29, 31, 33]. However, few studies have found significant relationships between *PRNP* polymorphisms and occurrence of BSE [28]. The number of BSE-affected animals tested in the present study (6 cattle) was too small for reliable estimation of genetic relationships between bovine *PRNP* polymorphisms and occurrence of BSE, and we found no evidence of such relationships.

In the present study, we assayed for *PRNP* polymorphisms in 863 healthy Holstein cattle and 186 healthy JB cattle. The only polymorphism caused amino acid substitutions in the ORF was the octapeptide repeat. We observed only 2 SNPs, at G234A and C576T; these SNPs have frequently been observed in other studies [8, 10, 13, 17, 28, 31]. Only 2 of the 863 Holstein cattle were heterozygous for the C576T polymorphism, whereas 91 of the 186 JB cattle were heterozygous at C576T (Table 2). Similar differences in allele frequencies between the 2 cattle breeds were found at the 23- and 12-bp indels and the G234A SNP. These differences may be due to inherent properties of the cattle breeds or differences in the breeding systems used for Holstein and JB cattle. The allele frequencies of the bovine *PRNP* gene observed in the present study for JB cattle suggest a breeding system in which a limited number of bulls is used. Takasuga *et al.* [31] found 13 SNPs (including 2 amino acid substitutions) in indigenous Indonesian cattle, which carry more mutations than Holstein and JB cattle. It is generally thought that artificial insemination, which is widely used to breed dairy and beef cattle, decreases genetic variation and produces uniform genetic properties at the DNA level. Holstein and JB cattle raised in Japan appear to have fewer mutation sites in the *PRNP* gene than indigenous breeds such as indigenous Indonesian cattle [31].

Several cattle breeds have been shown to have octarepeat polymorphisms in the ORF of the *PRNP* gene [5, 22, 25, 33], and 3 alleles of the octapeptide repeat (5, 6 and 7 copies) have been reported. In the present study, none of the cattle had 7 copies of the octapeptide repeat, and the frequency of the 5-copy allele was very low (Tables 1 and 2). The predominant genotype of the octapeptide repeat in the present Holstein and JB cattle was homozygosity of the 6-copy allele. Variability of the octapeptide repeat has not been found to correlate with incidence of BSE in cattle [5, 14, 23], and no BSE-affected cattle have been found to be homozygous for the 5-copy allele. We found no significant differences in the genotype distribution of the SNPs or octarepeat polymorphisms between healthy and BSE-affected Holstein cattle (Table 2).

In the present study, we investigated DNA polymorphisms in 2 regions upstream from the ORF: a 23-bp indel in the upper region of exon 1, and a 12-bp indel in intron 1 (Fig. 1). The available evidence suggests that polymorphisms in these regions affect transcription of the *PRNP* gene [15, 18, 21]. In a previous study, the 23-bp insertion was found to occur more frequently in healthy cattle than BSE-affected cattle [28]. Among Holstein cattle in Japan, the 23-bp insertion has been found to have a lower allele frequency than the 23-bp deletion. We speculated that polymorphism of the 12-bp indel might affect expression levels of the *PRNP* gene, because the indel is in the promoter region of intron 1 and contains a putative Sp1-binding consensus sequence [9, 15, 18, 19]. It has been reported that a GC-rich region and Sp1-binding sequence upstream of exon 1 are both important factors in PRNP transcription [1, 15, 18], but the effects of this Sp1 sequence in intron 1 are unclear. Further research is needed to clarify the effects of the12-bp indel on expression of the *PRNP* gene.

In the present study, we identified a *PRNP* gene mutant with a 288-bp deletion in the ORF (Figs. 1 and 2D), in a specimen from our DNA stock samples. A prion protein with such an internal deletion may confer resistance to prion disease infection or act as a dominant-negative mutant that inhibits prion propagation in the cell [17, 36]. Accurate determination of the distribution of this deletion could help clarify whether it has a preventive effect against prion disease. However, we did not detect this 288-bp deletion in the *PRNP* gene of any of the present 1049 cattle. Our stock DNA specimen with the 288-bp deletion in the *PRNP* gene was obtained from a calf (C928) with the calf form of sporadic bovine leucosis (SBL) [16]. SBL appears to be caused by a somatic mutation in immature pre-B cells, and it is unclear whether the malignant process of SBL is related to an internal deletion in the *PRNP* gene. If the internal deletion in the *PRNP* gene found in specimen C928 is caused by a somatic mutation that is related to the malignant transformation of SBL, it is unlikely that such a deletion would be found in healthy cattle. We examined the bovine *PRNP* gene from the other 7 specimens of SBL calves, but none of those specimens had the same deletion (data not shown).

In conclusion, we found an extremely small number of *PRNP* polymorphic sites in the 2 cattle breeds examined in the present study, and we found no association between these polymorphisms and BSE. Because the number of BSE-affected animals tested was small, further genetic investigations using many samples from BSE cattle can be useful for assessment of the risk of BSE in Japan.

ACKNOWLEDGMENTS. We wish to thank the staff of the slaughterhouse and dairy farms from which bovine blood samples were obtained. This study was partly supported by a grant from the Ministry of Health and a Grant-in-Aid for Science Research from the Ministry of Education, Science and Culture of Japan (17380180).

REFERENCES

1. Baybutt, H. and Manson, J. 1997. Characterisation of two promoters for prion protein (PrP) gene expression in neuronal